

A Bond Graph Model Validation of an Experimental Single Zone Building

A. Merabtine¹, S. Mokraoui¹, R. Benelmir¹ and N. Laraqi²

Abstract: Modeling of the thermal behavior of buildings needs effective strategies of analysis and tools. This is particularly true when conduction of heat through walls and/or slabs has to be properly taken into account. This article is concerned with a new modeling strategy for solving the transient heat conduction equation in a finite medium (with extensive background application to the different elements of a building structure). The developed approach is based on the Bond Graph technique, a graphical modeling language which is particularly suitable to the treatment of problems involving energy transfer. With this model, two typical transient heat conduction situations (corresponding to the most practical cases in building envelope, such as heat transfer through vertical walls, roofs and slabs), are considered. The related validation procedure consists of comparing the obtained results with available analytical solutions. The Bond Graph technique is then used to model the dynamic thermal behavior over a single zone building structure. Finally, results are compared with a set of experimental data.

Keywords: Bond Graph, transient heat conduction, plane wall, simulation, building.

Nomenclature

A	surface of the constructive element, [m ²]
C	thermal capacity, [J.K ⁻¹]
c	specific heat, [J.kg ⁻¹ .K ⁻¹]
e	effort variable
f	flow variable
L	thickness, [m]
h_i, h_e	inside and outside convective coefficients, [W.m ⁻² .K ⁻¹]
k	thermal conductivity, [W.m ⁻¹ .K ⁻¹]

¹ Lorraine Univ. – Fac. Sc. Tech. - LERMAB, Vandoeuvre-les-Nancy, F54506, France

² Paris Ouest University, GTE Department, Lab. TIE, Ville d'Avray , F92410, France

Q	heat rate, [J]
\dot{Q}	heat flow, [W]
R	thermal resistance inside the wall, [K.W ⁻¹]
R_{cvi}, R_{cve}	inside and outside thermal resistances, [K.W ⁻¹]
Se	temperature source, [K]
T	temperature [K]
V	volume, [m ³]

Subscripts

0	initial
<i>cve</i>	outside convection
<i>cvi</i>	inside convection
<i>e</i>	external
<i>i</i>	internal
<i>in</i>	entering
<i>l</i>	layer
<i>W</i>	wall

Symbols

α	diffusivity [m ² .s ⁻¹]
β	eigenvalue
ρ	density, [kg.m ⁻³]

1 Introduction

The “envelope” is one of the most important sub-systems affecting energy efficiency of a building. Proper building thermal modeling requires therefore accurate descriptions/characterization of the building envelope components. The heating loads of the buildings depend on the thermal transmittance of envelope components, mainly the transmittance by heat conduction through walls, roofs and floors. Hence, in order to evaluate heat storage and losses, transient heat conduction through walls has become an area of interest in building-related disciplines. This trend has been motivated by the fast development of computer technology which allows solving such problems quickly and accurately. In fact, with increasing capacity of computers, dynamic thermal modeling of building has been intensively investigated.

The first attempts of dynamic simulation were analogical models consisting of real resistors and capacitors. The advantage of this approach was simplicity and higher computational speed comparing with models running in computers of early stage. Afterward, several approaches such as finite difference methods and direct analytical methods emerged making modeling more and more complicated and even more CPU time consuming. That is why an interesting category of alternative models, called *Grey box models*, has been developed and has become over the years the focus of several investigations.

Grey box models are based on physical laws and an identification procedure using a limited number of parameters having a definite physical meaning. The thermal network model using electrical analogy parameters is an example of grey box models. Grey box models can represent the physical properties of the building system and predict its thermal behavior and consumption. Hence, they are suitable for the treatment of nonlinear processes such as solar radiation. They are considered as simplified physical models which can represent properly the physical properties of the building system.

Among the several grey box models, Déqué, Olivier and Poblador (2000) developed a grey box model that can predict the thermal behavior and energy consumption of buildings starting from a minimum of geometrical and physical parameters. Their model gives emphasis, especially, to the technological approach by ensuring the visibility of the physical system. This feature provides a high flexibility. Lorenz and Massy (1985), Tindale (1993) and Gouda, Danaher and Underwood (2002) used the lumped-parameters method involving the break-up of construction elements into a number of uniform temperature elements about which an energy balance can be expressed. A nonlinear constrained optimization method has been used for reducing the model order of building elements by Gouda, Danaher and Underwood (2002).

Another methodology belonging to the *white box modeling* technique consists of the use of a graphical language by means of a simplified graphical modeling tool. This model is based on the Bond Graph approach. This approach has the potential to display explicitly the nature of power in a building system, such as a phenomenon of storage, processing and dissipating energy. In particular, this approach responds well to the needs of dynamic modeling of the building with respect to the following characteristics:

- an energetic approach that allows a decomposition of the building into sub-systems that exchange power;
- a graphical representation in order to visualize the power transfer and the related causality;

- an inherent flexibility easing model extension, allowing consideration of other details not taken into account at the first stage of modeling;
- writing systematic mathematical differential equations from the Bond Graph model.

In thermal building design, this method has been used, mainly, by Cellier and Nebot (2006) and Weiner and Cellier (1993). In their studies, the results seem to be similar to those obtained with the analysis tools DOE-2 and CALPAS 3. The same findings have been given by Yu and Van Passeen (2004) when they compare the Bond Graph results with those of Matlab-Simulink tools.

It is worth noting, that in the Bond Graph methodology, as in several white box models, the modeling approach involves four distinctive levels. The *technological level* is a construction of the architecture of the system through the assembly of components, which can be identified in the “real” system (heat exchanger, walls, radiator . . .). In the *physical level*, the modeling uses an energy description of the physical phenomena based on fundamental concepts of physics in which the internal physical mechanisms are specified in order to describe the behavioral aspects of the system. For instance, dissipation, transformation, storage of energy are physical aspects of a thermal system. In the *mathematical level*, we specify the exact nature of the relations between variables, parameters, constants by the use of mathematical equations which describe the system behavior. Finally, the *algorithmic level* allows solving the mathematical equation to simulate and analyze the system behavior.

In this article, we describe how Bond Graph approach can be used to model conduction heat transfer in plane walls with the objective of providing the best modeling scheme. In section 2, a representation of the Bond Graph methodology is carried out. Next, the Bond Graph model for two cases study regarding the boundary conditions type is developed in section 3. Section 4 provides the analytical solution for the above mentioned cases. Finally, a comparison between the results of Bond Graph and analytical models is carried out in section 5, followed by a building case study with a validation of the Bond Graph model by means of experimental results.

2 Bond Graph methodology

The Bond Graph technique is based on a graphical formalism. It is well suited for modeling physical processes and multidisciplinary dynamic engineering systems including features and components involved in different energy domains [Borutzky (2010)]. Its philosophy is founded on a systematic and common way representation of power flow between the model’s components. Paynter (1961) pioneered

the Bond Graph formalism and used it for modeling dynamic multiport systems. He suggested that energy and power are the fundamental dynamic variables which characterize all physical interactions.

In Bond Graph modeling, the interaction between two components is modeled by a bond with a semi-arrow at the end. The power is represented as a product of two physical quantities, one extensive, the other intensive. These two power conjugated variables are called *effort* and *flow* and are denoted by the letters e and f (Fig. 1).



Figure 1: Bond Graph link representation.

The selection of the two physical quantities is specific for each physical domain. For instance, in electrical domain, we use the voltage u as an effort variable and the current i as flow variable. In thermal domain, the effort variable is represented by a temperature T and the flow variable by an entropy flow \dot{S} .

A classification of Bond Graph elements can be made up by the number of “ports”; ports are placed where interactions with other processes take place. There is one port elements symbolizing inertial element (I), capacitive element (C), resistive elements (R), effort source (Se) and flow source (Sf), and two ports elements representing transformer element (TF) and gyrator element (GY). The elements I, C, and R are passive elements because they convert the supplied energy into stored or dissipated energy. The sources Se and Sf are active elements because they supply power to the system. The bonds are inter-linked by two type junction elements (0 and 1-junctions) which serve to connect I, C, R, and source elements. At the 0-junction the flow adds up to zero while all efforts are equal, and at the 1-junction all effort variables add up to zero while all flows are equal. The causality is an important concept embedded in Bond Graph theory. This refers to cause and effect relationship. Causality assignment is implicitly introduced [Karnopp and Rosenberg (1990)].

Causality assignment is independent of the power flow direction. This leads to the description of Bond Graph in the form of state – space equation. The sources (Se and Sf) have fixed causality, the dissipative element (R) has free causality depending on the causality of the other elements of Bond Graph, and the storage elements (I and C) have preferential causality, that is integral causality or derivative causality, but it is always desirable that C and I elements be in integral causality. Transformer, gyrator and junction elements have constrained causality.

As explained previously, the power variables of the thermal system are the temperature T and the entropy flow \dot{S} , but it is known that entropy flow cannot be measured directly [Nebot and Cellier (1999)]. It is easier to use heat flow \dot{Q} as flow variable which is a measurable variable. However, a product of temperature and heat flow is not the power transferred between ports. This has led researchers to introduce pseudo-Bond Graph method. Their advantage is that modeling of thermal systems becomes easier.

3 The Bond Graph method for solving transient heat conduction problems

In this section, we present the Bond Graph method used for solving one-dimensional unsteady heat conduction problem in a finite medium subject to asymmetric, time-independent, boundary conditions. We consider two cases: (i) the case of a plane wall with two different convective conditions at each surface boundary of the wall; and (ii) the case of the wall with one convective condition at one surface boundary, the second surface being maintained at constant temperature. Generally, these are the two main types of boundary conditions encountered in problems of thermal building.

In the first case (Fig. 2), the absolute temperature T may be chosen as an effort variable and the heat flow as a flow variable.

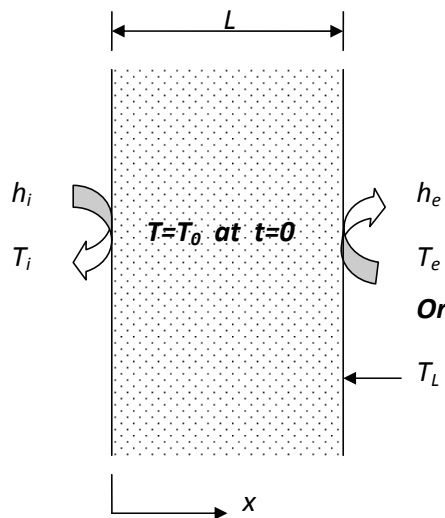


Figure 2: Representation of the heat transfer problem through the wall.

The so-called “lumped parameter” assumption is usually adopted for this kind of

cases. This is realized by splitting the wall into a number of layers, where, temperature and thermo-physical properties are assumed homogeneous. Each layer stores and conducts heat simultaneously. The external layers are subjected to convection heat exchange with inside and outside surrounding.

Thus, the word pseudo Bond Graph representation of heat conduction through the wall constituted of four layers is shown in Figure 3. This figure indicates the technological level of modeling.

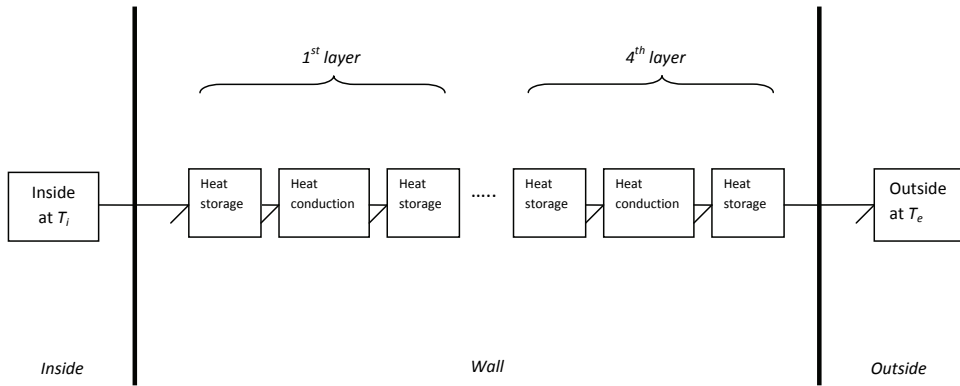


Figure 3: Word pseudo-Bond Graph representation of the wall

In Figure 4, the physical level of modeling by a Bond Graph is pointed out. Inside and outside temperatures, T_i and T_e , are modeled by the effort sources S_{e1} and S_{e1} . The convective boundary conditions are represented by two 1-junctions $1_{1,2,3}$ and $1_{22,23,24}$ related respectively to the resistance elements R_{cvi} and R_{cve} representing the inside and outside resistances to heat transfer by convection. These two 1-junctions are characterized by equality to zero of the sum of effort variables (temperatures). Therefore the following relations are obtained:

$$T_1 = T_2 + T_3 \text{ or } T_i = T_2 + T(0, t) \tag{1}$$

$$T_{22} = T_{21} + T_{23} \text{ or } T_{22} = T(L, t) - T_e \tag{2}$$

In Bond Graph modeling, the constitutive equation related to R-elements is: $f = \frac{e}{R}$. Thus, the dynamic equations of the two resistance elements R_{cvi} and R_{cve} are given by

$$f_2 = \frac{e_2}{R_2} \Rightarrow \dot{Q}_2 = \frac{T_2}{R_2} = \frac{T_i - T(0, t)}{R_{cvi}} = \dot{Q}_i \tag{3}$$

$$f_{22} = \frac{e_{22}}{R_{22}} \Rightarrow \dot{Q}_{22} = \frac{T_{22}}{R_{22}} = \frac{T(L,t) - T_e}{R_{cve}} = \dot{Q}_e \tag{4}$$

Where $R_{cvi} = \frac{1}{h_i A}$ and $R_{cve} = \frac{1}{h_e A}$.

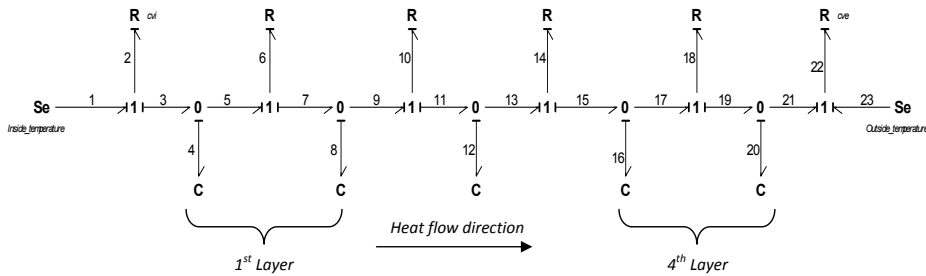


Figure 4: Pseudo-Bond Graph model of the wall

Through boundary surfaces of the wall, the heat flow entering and leaving the wall are represented by two 0-junctions: $0_{1,2,3}; 0_{20,21,22}$ characterized by the equality to zero of the sum of flow variable (heat flow). The effort variables are equal for each of those junctions. For each layer inside the wall, the heat quantity is decomposed into two parts: the first part is dissipated by conduction; modeled by a 1-junction related to R-element representing the conductive resistance, whereas the second part is stored by the layer; modeled by a 0-junction related to C-element representing the thermal capacity. Then the dynamic equations for those junctions are given by

For 1st layer:

$$\left\{ \begin{array}{l} 0_{3,4,5} : \begin{cases} \dot{Q}_4 = \dot{Q}_3 - \dot{Q}_5 = \dot{Q}_i - \dot{Q}_5 \\ T_3 = T_4 = T_5 = T(0,t) \end{cases} \\ 1_{5,6,7} : \begin{cases} \dot{Q}_5 = \dot{Q}_6 = \dot{Q}_7 \\ T_6 = T_5 - T_7 \end{cases} \\ 0_{7,8,9} : \begin{cases} \dot{Q}_8 = \dot{Q}_7 - \dot{Q}_9 \\ T_8 = T_7 = T_9 \end{cases} \end{array} \right. \tag{5}$$

For 2nd layer:

$$\left\{ \begin{array}{l} 0_{7,8,9} : \begin{cases} \dot{Q}_8 = \dot{Q}_7 - \dot{Q}_9 \\ T_8 = T_7 = T_9 \end{cases} \\ 1_{9,10,11} : \begin{cases} \dot{Q}_9 = \dot{Q}_{11} - \dot{Q}_{13} \\ T_{10} = T_9 - T_{11} \end{cases} \\ 0_{11,12,13} : \begin{cases} \dot{Q}_{12} = \dot{Q}_{11} - \dot{Q}_{13} \\ T_{11} = T_{12} = T_{13} \end{cases} \end{array} \right. \quad (6)$$

For 3rd layer:

$$\left\{ \begin{array}{l} 0_{11,12,13} : \begin{cases} \dot{Q}_{12} = \dot{Q}_{11} - \dot{Q}_{13} \\ T_{11} = T_{12} = T_{13} \end{cases} \\ 1_{13,14,15} : \begin{cases} \dot{Q}_{13} = \dot{Q}_{14} - \dot{Q}_{15} \\ T_{14} = T_{13} - T_{15} \end{cases} \\ 0_{15,16,17} : \begin{cases} \dot{Q}_{16} = \dot{Q}_{15} - \dot{Q}_{17} \\ T_{15} = T_{16} = T_{17} \end{cases} \end{array} \right. \quad (7)$$

For 4th layer:

$$\left\{ \begin{array}{l} 0_{15,16,17} : \begin{cases} \dot{Q}_{16} = \dot{Q}_{15} - \dot{Q}_{17} \\ T_{15} = T_{16} = T_{17} \end{cases} \\ 1_{17,18,19} : \begin{cases} \dot{Q}_{17} = \dot{Q}_{18} - \dot{Q}_{19} \\ T_{18} = T_{17} - T_{19} \end{cases} \\ 0_{19,20,21} : \begin{cases} \dot{Q}_{20} = \dot{Q}_{19} - \dot{Q}_{21} = \dot{Q}_{19} - \dot{Q}_e \\ T_{19} = T_{20} = T_{21} = T(L,t) \end{cases} \end{array} \right. \quad (8)$$

The constitutive equations corresponding to R and C-elements inside the wall are expressed as:

For C elements: $e_k = \frac{1}{C_k} \int_0^t f_k dt + e_k(0)$

$$T_4 = \frac{1}{C_4} \int_0^t \dot{Q}_4 dt + T_4(0) \quad (9)$$

$$T_8 = \frac{1}{C_8} \int_0^t \dot{Q}_8 dt + T_8(0) \quad (10)$$

$$T_{12} = \frac{1}{C_{12}} \int_0^t \dot{Q}_{12} dt + T_{12}(0) \quad (11)$$

$$T_{16} = \frac{1}{C_{16}} \int_0^t \dot{Q}_{16} dt + Q_{16}(0) \quad (12)$$

$$T_{20} = \frac{1}{C_{20}} \int_0^t \dot{Q}_{20} dt + Q_{20}(0) \quad (13)$$

For R elements: $f_k = \frac{e_k}{R_k}$

$$\dot{Q}_6 = \frac{T_6}{R_6} \quad (14)$$

$$\dot{Q}_{10} = \frac{T_{10}}{R_{10}} \quad (15)$$

$$\dot{Q}_{14} = \frac{T_{14}}{R_{14}} \quad (16)$$

$$\dot{Q}_{18} = \frac{T_{18}}{R_{18}} \quad (17)$$

Where: C_4, C_8, C_{12}, C_{16} and C_{20} are thermal capacities for each layer;

$$C_4 = C_8 = C_{12} = C_{16} = C_{20} = \frac{C_W}{5} \quad (18)$$

And $C_W = \rho V c$ is the heat capacity of the wall,

with, ρ denotes the density, V the volume and c the specific heat capacity.

R_6, R_{11}, R_{14} and R_{19} are the conductive resistances for each layer;

$$R_6 = R_{11} = R_{14} = R_{19} = \frac{R_W}{4} \quad (19)$$

$R_W = \frac{L}{kA}$ is the global conductive resistance for the wall.

Next, we derive the following system of differential equations:

$$\left\{ \begin{array}{l} \frac{dT_4}{dt} = \frac{5\dot{Q}_4}{C_W} = \frac{5}{C_W} \left[\frac{T_1 - T_4}{R_{cvi}} - \frac{4(T_4 - T_7)}{R_W} \right] \\ \frac{dT_8}{dt} = \frac{5\dot{Q}_8}{C_W} = \frac{5}{C_W} \left[\frac{4(T_4 - T_8)}{R_W} - \frac{4(T_8 - T_{12})}{R_W} \right] \\ \frac{dT_{12}}{dt} = \frac{5\dot{Q}_{12}}{C_W} = \frac{5}{C_W} \left[\frac{4(T_8 - T_{12})}{R_W} - \frac{4(T_{12} - T_{16})}{R_W} \right] \\ \frac{dT_{16}}{dt} = \frac{5\dot{Q}_{16}}{C_W} = \frac{5}{C_W} \left[\frac{4(T_{12} - T_{16})}{R_W} - \frac{4(T_{16} - T_{20})}{R_W} \right] \\ \frac{dT_{20}}{dt} = \frac{5\dot{Q}_{20}}{C_W} = \frac{5}{C_W} \left[\frac{4(T_{16} - T_{20})}{R_W} - \frac{T_8 - T_{12}}{R_{cve}} \right] \end{array} \right. \quad (20)$$

At this stage, $T(0, t)$, $T(L, t)$, \dot{Q}_i and \dot{Q}_e can be evaluated by using the above equations respecting the integral causality.

In the second case, associated to the case of heat transfer through a roof a building, the same approach is used. At $x = L$, we fix the temperature T_L . In Bond Graph model, this condition is approximated by tending the convection coefficient h_e toward infinity, i.e. R_{cve} becomes negligible, hence, the effort source S_e corresponding to the outside temperature becomes equal to T_L .

4 Analytical solution

We consider a heat conduction problem in a one-dimensional finite region, as illustrated in Figure 2. We use the separation of variables method (see [Özisik (1993)]). Among various available methods to solve this kind of problems, there is the method of separation of variables which is most effective and straightforward to apply when both the differential equation and boundary conditions are homogenous. In our case, we have non-homogenous boundary conditions, then, a direct application of separation of variables method is not possible. In many cases, a non-homogenous problem can be split up into several simpler problems. In our case, we shall split this problem into two parts:

- a steady-state problem defined by the temperature variable $U(x)$;
- a homogenous time-dependent problem defined by the temperature variable $V(x, t)$

Consequently, the temperature $T(x, t)$ is expressed as

$$T(x, t) = U(x) + V(x, t) \quad (21)$$

Case 1: Heat conduction in a wall with convective conditions on both sides. The mathematical formulation of this problem is as follows:

Energy balance

$$\frac{\partial^2 T}{\partial x^2} = \frac{1}{\alpha} \frac{\partial T}{\partial t} \quad (22)$$

for $0 < x < L, t > 0$.

Initial condition

$$T(x, t) = T_0 \quad (23)$$

for $t = 0, 0 \leq x \leq L$.

Boundary conditions

$$-k \frac{\partial T}{\partial x} = h_i [T_i - T] \quad (24)$$

for $x = 0, t > 0$.

$$-k \frac{\partial T}{\partial x} = h_e [T - T_e] \quad (25)$$

for $x = L, t > 0$.

Substituting Equation (21) into equations (22-25) leads to the following two sub-systems

Sub-problem 1:

Energy balance

$$\frac{\partial^2 U}{\partial x^2} = 0 \quad (26)$$

for $0 < x < L, t > 0$.

Boundary conditions

$$-k \frac{\partial U}{\partial x} = h_i (U - T_i) \quad (27)$$

for $x = 0, t > 0$.

$$-k \frac{\partial U}{\partial x} = h_e (U - T_e) \quad (28)$$

for $x = L, t > 0$.

Sub-problem 2:

Energy balance

$$\frac{\partial^2 V}{\partial x^2} = \frac{1}{\alpha} \frac{\partial V}{\partial t} \quad (29)$$

for $0 < x < L, t > 0$.

Initial condition

$$V(x, t) = T_0 - U(x) \quad (30)$$

for $t = 0, 0 \leq x \leq L$.

Boundary conditions

$$k \frac{\partial V}{\partial x} = h_i \cdot V \tag{31}$$

for $x = 0, t > 0$.

$$-k \frac{\partial V}{\partial x} = h_e \cdot V \tag{32}$$

for $x = L, t > 0$.

The solution of equation (26) is straightforward

$$U(x) = Ax + B \tag{33}$$

Where parameter A and B , are determined using the boundary conditions of equations (27-28). Thus,

$$A = \frac{T_e - T_i}{L + \frac{1}{H_e} + \frac{1}{H_i}}; \quad B = T_i + \frac{T_e - T_i}{1 + H_i L + \frac{H_i}{H_e}}$$

Where, $H_i = \frac{h_i}{k}$ and $H_e = \frac{h_e}{k}$.

The second sub-problem can be now treated using separation of variable methods.

Assume temperature $V(x,t)$ have the following form

$$V(x,t) = \Psi(x)\Gamma(t) \tag{34}$$

Where, $\Psi(x)$ is a space function and $\Gamma(t)$ is a time function

Equation (29) becomes

$$\frac{1}{\Psi} \left(\frac{d^2 \Psi}{dx^2} \right) = \frac{1}{\alpha \Gamma} \frac{d\Gamma}{dt} = -\beta^2 \tag{35}$$

Then, the separated function $\Gamma(t)$ satisfies the equation

$$\frac{\partial \Gamma(t)}{\partial t} + \alpha \beta^2 \Gamma(t) = 0 \tag{36}$$

This gives us the following solution :

$$\Gamma(t) = e^{-\alpha \beta^2 t} \tag{37}$$

The space variable function $\Psi(\beta, x)$ satisfies the following eigenvalue problem

$$\frac{\partial^2 \Psi(x)}{\partial x^2} + \beta^2 \Psi(x) = 0 \tag{38}$$

for $0 < x < L, t > 0$.

Boundary conditions

$$-\frac{\partial \Psi(x)}{\partial x} + H_i \cdot \Psi(x) = 0 \tag{39}$$

for $x = 0, t > 0$.

$$\frac{\partial \Psi(x)}{\partial x} + H_e \cdot \Psi(x) = 0 \tag{40}$$

for $x = L, t > 0$.

The general solution of equation (38), under boundary conditions (39-40), yields the following eigenfunctions $\Psi(\beta_m, x)$:

$$\Psi(\beta_m, x) = \beta_m \cos(\beta_m x) + H_i \sin(\beta_m x) \tag{41}$$

where, the positives eigenvalues β_m are the roots of the following transcendental equation

$$\tan(\beta_m L) = \frac{\beta_m (H_i + H_e)}{\beta_m^2 - H_i H_e}, \quad (m = 1, \infty) \tag{42}$$

Knowing the eigenfunctions and the eigenvalues, the solution for the variable $V(x,t)$ is given in the form:

$$V(x,t) = \sum_{m=1}^{\infty} \frac{C_m}{N_m} \Psi(\beta_m, x) e^{-\alpha \beta_m t} \tag{43}$$

Where, according to the orthogonality property of the eigenfunctions, it follows:

$$N_m = \int_0^L [\Psi(\beta_m, x)]^2 dx \tag{44}$$

with, N_m is Norm of the eigenfunction.

Applying the initial condition of equation (30) and multiplying its hand and left sides by $\Psi(\beta_m, x)$, we get, after integration with respect to x variable, the following form for C_m :

$$C_m = \int_0^L (T_o - U(x)) \cdot \Psi(\beta_m, x) dx \tag{45}$$

The Integrals in equations (44) and (45) are developed:

$$N_m = \frac{1}{2} \left[(\beta_m^2 + H_i^2) \left(L + \frac{H_e}{\beta_m^2 + H_e^2} \right) + H_i \right] \quad (46)$$

$$C_m = \sin(\beta_m L) \left[T_0 - B - A \left(L + \frac{H_i}{\beta_m^2} \right) \right] - \cos(\beta_m L) \left[\frac{A}{\beta_m} + \frac{H_i}{\beta_m} (T_0 - AL - B) \right] + \frac{A}{\beta_m} + \frac{H_i}{\beta_m} (T_0 - B) \quad (47)$$

Finally, the complete solution for the temperature $T(x, t)$ is expressed in the form:

$$T(x, t) = (Ax + B) + \sum_{m=1}^{\infty} \frac{C_m}{N_m} \Psi(\beta_m, x) e^{-\alpha \beta_m^2 t} \quad (48)$$

Case 2: Heat conduction in a wall with convective condition on one side and fixed temperature on the other side, the mathematical formulation is as follows:

Energy balance

$$\frac{\partial^2 T}{\partial x^2} = \frac{1}{\alpha} \frac{\partial T}{\partial t} \quad (49)$$

for $0 < x < L, t > 0$.

Initial condition

$$T(x, t) = T_0 \quad (50)$$

for $t = 0, 0 \leq x \leq L$.

Boundary conditions

$$-k \frac{\partial T}{\partial x} = h_i [T_i - T] \quad (51)$$

for $x = 0, t > 0$.

$$T(x, t) = T_L \quad (52)$$

for $x = L, t > 0$.

Using the same methodology as in case 1, we obtain the following equations.

The complete solution for $T(x, t)$ is:

$$T(x, t) = (Ax + B) + \sum_{m=1}^{\infty} \frac{C_m}{N_m} \Psi(\beta_m, x) e^{-\alpha \beta_m^2 t} \quad (53)$$

The eigenfunctions $\Psi(\beta_m, x)$, the norm N_m and the parameter C_m take the form:

$$\Psi(\beta_m, x) = \sin(\beta_m(L - x)) \quad (54)$$

$$N_m = \frac{1}{2} \left[\frac{L(\beta_m^2 + H_i^2) + H_i}{\beta_m^2 + H_i^2} \right] \quad (55)$$

$$C_m = \frac{1}{\beta_m} [T_0 - AL - B - (T_0 - B) \cos(\beta_m L)] + \frac{A}{\beta_m^2} \sin(\beta_m L) \quad (56)$$

The eigenvalues β_m are obtained from the following characteristic equation:

$$\cot(\beta_m L) = -\frac{H_i}{\beta_m} \quad (57)$$

and the parameters A and B have the following expression:

$$A = \frac{1}{L} \left[T_L - \frac{H_i T_i L + T_L}{H_i L + 1} \right]; B = \frac{H_i T_i L + T_L}{H_i L + 1}$$

5 Simulation results

5.1 Validation

In this section, the performed simulations of transient heat conduction through walls will be illustrated by calculating the surface temperatures, heat fluxes and energy stored quantities.

The thermo – physical and geometric characteristics of the chosen wall are presented in table 1. This table includes also the boundary conditions values.

In order to validate our pseudo-Bond Graph model, we have compared all simulation results with those of analytical method. Figure 5a exhibits the results of temperature variations with time for three positions in the wall ($x = 0$ m; 0.1 m and 0.2 m). It shows that there is a good agreement between Bond Graph model and both analytical calculations. Figure 5b indicates the magnitude of absolute deviations on the calculated temperatures between Bond Graph model and analytical method. It can be observed that the maximum of deviations occurs at the first hours then tend towards zero, for each position in the wall, after about 20 hours of simulation.

The pseudo-Bond Graph determined profiles of heat stored and heat flow leaving and entering the plane wall are compared in Figures 6a and 6b with their analytical counterparts. Agreement between the two simulation results is shown to be satisfactory. The steady state is reached after 20 hours of simulation. Furthermore, these graphs clearly illustrate the fact that the heat flow leaving is more important than the heat flow entering the wall. This can be explained by the important temperature gradient between the outside and the wall ($[T_e - T(L, t)] > [T_i - T(0, t)]$).

Table 1: Characteristics data of the studied heat conduction problems

Geometric parameters	Wall Thickness; L (m)	0.2
	Wall heat transfer section; A (m^2)	1
Thermo-physical parameters	Wall material	Concrete block
	Thermal Conductivity; k ($W.m^{-1}.K^{-1}$)	0.963
	specific Heat capacity; c ($J.Kg^{-1}.K^{-1}$)	650
	Density; ρ ($Kg.m^{-3}$)	1300
Inside and outside conditions	Inside convection coefficient; h_i ($W.m^{-2}.K^{-1}$)	3
	Outside convection coefficient; h_e ($W.m^{-2}.K^{-1}$)	17.8
	Inside temperature; T_i ($^{\circ}C$)	21
	Wall : Outside temperature; T_e ($^{\circ}C$)	0
	Fixed end temperature; T_L ($^{\circ}C$)	12
	Initial temperature; T_0 ($^{\circ}C$)	12

Moreover, the heat stored by the wall (or, in this case, evacuated) decreases to reach a value of $-1.08 MJ/m^2$ at the steady state.

Results related to the heat conduction in the wall subject to a fixed temperature condition in one side and one convective condition on the other are depicted hereafter. Temperature profiles plots, for three different positions in the wall ($x=0 m$; $x=0.1 m$; $x=0.2 m$), are shown in Figure 7a. The corresponding deviations plots, between analytical and Bond Graph methods, on the calculated temperatures are presented in Figure 7b. Obviously, good agreement can be observed between the analytical predictions and those obtained by the pseudo Bond Graph model. From Figure 7a, we can analyze the thermal behavior of the wall. Indeed, the achieved steady state temperature decreases more and more when going away from inside surface boundary to the outside one. Upon observing Figure 7b, it can be noticed that the deviations on the calculated temperature does not exceed ± 0.4 $^{\circ}C$ for the boundary surface $x = 0 m$ and ± 0.025 $^{\circ}C$ for $x = 0.1 m$.

Thereafter, the heat stored into the wall, as well as the heat flows entering and

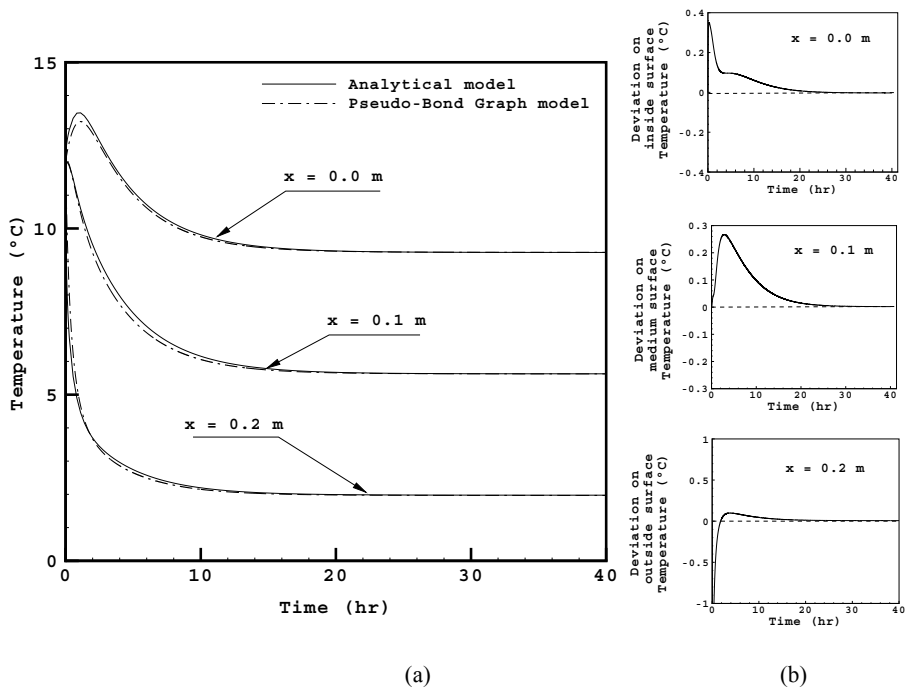


Figure 5: Temperature profiles in the wall (a) and the corresponding absolute deviations between Bond Graph model and analytical method (b). (case1: two convective boundary conditions)

leaving the wall is illustrated in Figure 8. From figure 8b, the leaving flows (heat losses) decrease rapidly at the first times then increase gradually with time before reaching the steady-state. Alternatively, the entering flows (heat gains) decrease continually until reaching the same steady-state. It is also indicated, from Figure 8a, that the heat stored by the wall decreases firstly then increases with time because the inside gradient of temperature $[T_i - T(0,t)]$ becomes more important than the outside one. However, for the first moments, the calculated Bond Graph heats and flux show some disparities with the analytical ones. Upon comparing these results it can be stated that the pseudo-Bond Graph model agrees accurately with the analytical method.

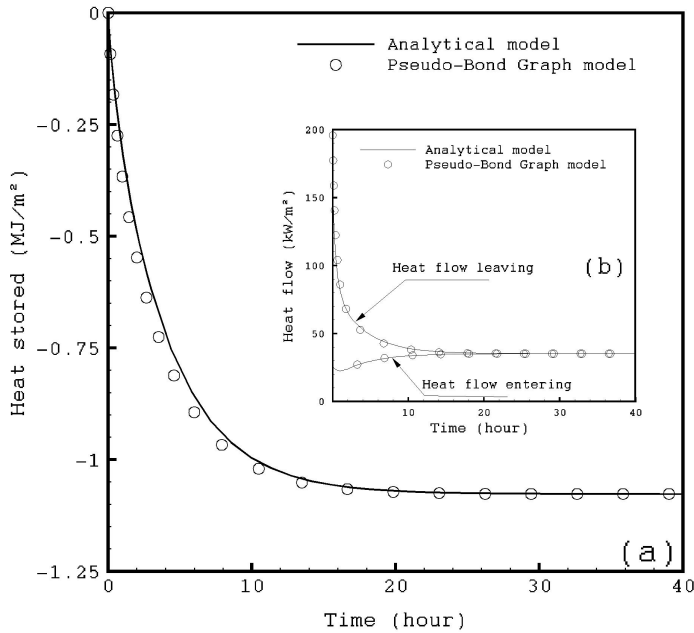


Figure 6: Heat stored by the wall (a) and heat flows leaving and entering the wall (b). (case1: two convective boundary conditions)

5.2 Test case

The experimental building is a workshop space of 2050 m² assimilated to a single-zone building located in Nancy (France). It is a heated space with the following dimensions: 9 × 25 × 82 m (height × width × length). Table 2 presents the building envelope material properties.

In table 2, the U-value coefficients are calculated including the internal and external heat transfer coefficients, which have respectively the values of 3 and 17 W/m²K.

The heating system consists of a natural gas boiler allowing up to 200 kW of heat-rate. The heat supply is insured by 8 air heaters. The temperature is controlled by means of a thermostatic valve system and a temperature sensor located at each blowing orifice of the air heaters. In order to validate our model, accurate temperature measurements have been performed during three successive days through a platinum resistance sensor which provides results with an uncertainty not higher than ± 0.01 K. During the tests, the set-point temperature is fixed to 17 °C for day time (from 08 00 am to 08 00 pm) and 15 °C for night time. The local is unoccupied

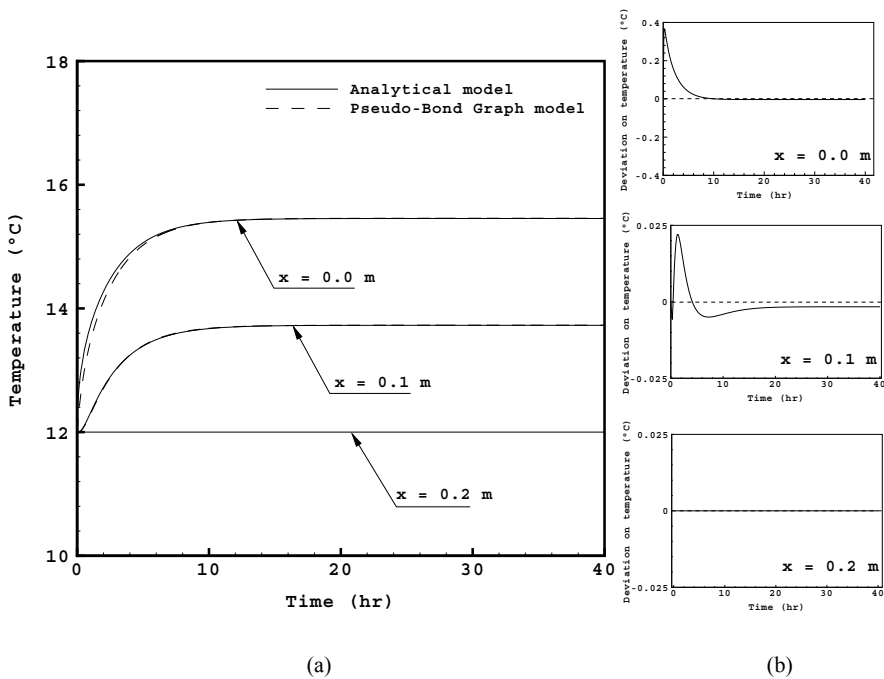


Figure 7: Temperature profiles in the wall (a) and the corresponding absolute deviations between Bond Graph model and analytical method (b). (case2: one convective and one fixed temperature conditions at each boundary)

and we consider that solar gain is negligible because of closing windows during this period. The exterior temperature variation file has been generated by means of a local weather station providing maximum and minimum temperatures of the day.

The model of the present building invokes smaller models (sub-models) that are related to the constructive elements of the building: external walls, roof and slab.

First, the sub-models have been created to describe the physics of heat transfer considering conduction and convection. Heat flow through these elements is affected by convection and conduction phenomena as well as by outdoor/indoor temperature difference.

In the next step, all elements at the boundaries of the building are connected to the thermal capacity C_{zone} which takes the form:

$$C_{zone} = \rho_{air} \times V_{building} \times c_{air} \quad (58)$$

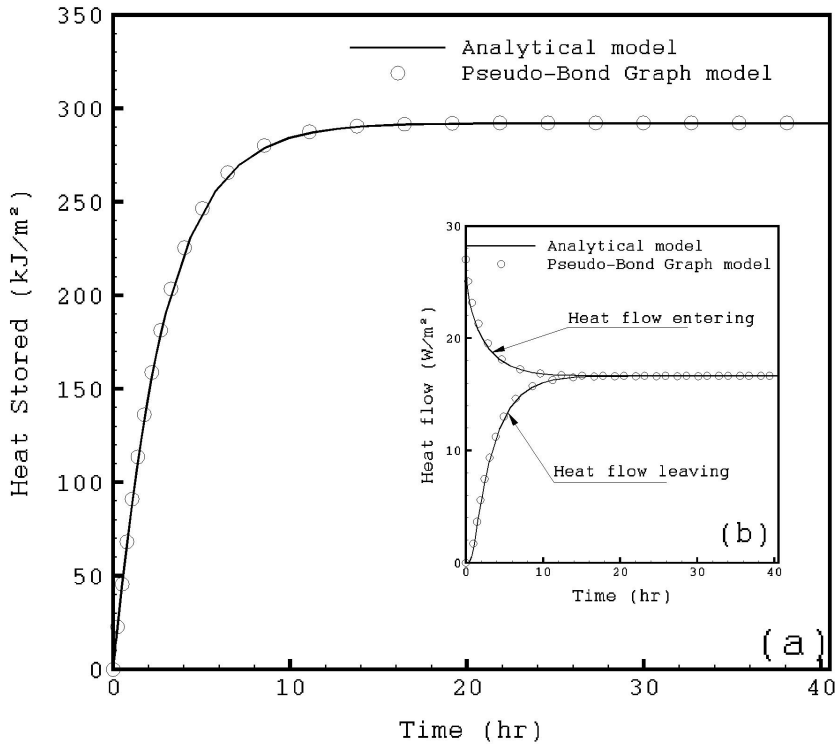


Figure 8: Heat stored by a wall (a) and heat flows leaving and entering the wall (b). (case2: one convective and one fixed temperature conditions at each boundary)

The PID controller drives the heating process in order to minimize the difference between the indoor set and measured temperatures. The pseudo-Bond Graph of the building can be represented in Figure 9.

Pseudo-Bond Graph model was run using measured weather data for three successive days of the winter period (February 5th to 7th, 2009). Heating loads are calculated and compared between the two models and a comparison against measured indoor temperature is carried out. Figure 10 represents the distribution of the outdoor temperature, the set point temperature and the measured indoor temperature.

The set point temperature is fixed to 15 °C for night time and 17 °C for day time, whereas, the outdoor temperature fluctuates between the minimum and the maxi-

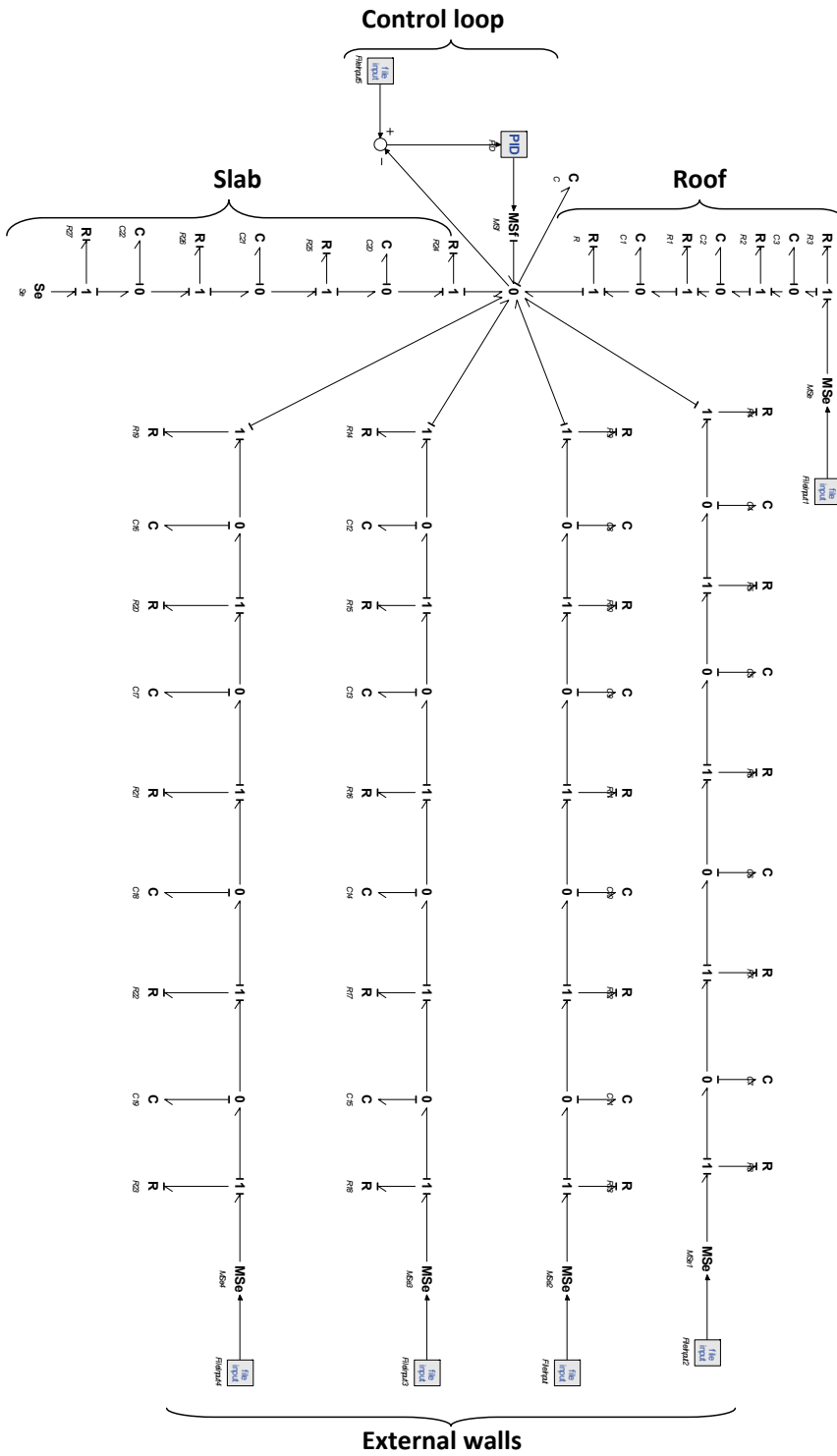


Figure 9: The pseudo-Bond Graph model of the building

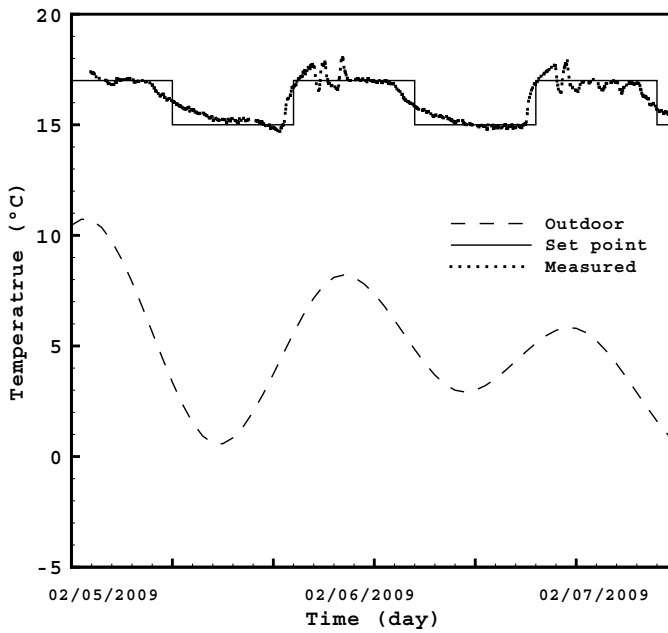


Figure 10: Outdoor, set point and measured indoor temperatures

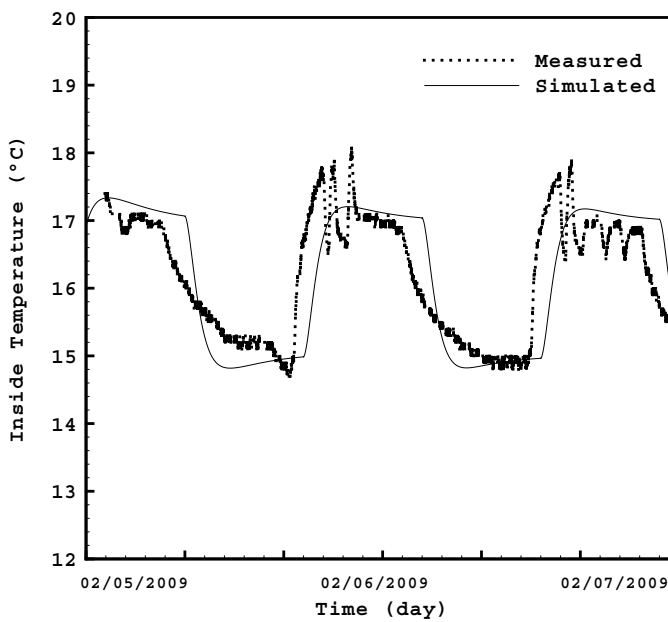


Figure 11: Comparison between measured and simulated indoor temperature data

Table 2: Material specifications of the building

Material	Thermal conductivity	Thickness	U value
	($\text{W}\cdot\text{m}^{-1}\cdot\text{K}^{-1}$)	(m)	($\text{W}\cdot\text{m}^{-2}\cdot\text{K}^{-1}$)
Exterior wall (inside to outside)			0.433
Concrete block	1.05	0.2	
Rock wool	0.04	0.08	
Steel	46	0.001	
Roof (inside to outside)			0.477
Asbestos-cement	0.95	0.075	
Glass wool	0.04	0.075	
Bituminous roofing	0.5	0.01	
Floor			3.522
Concrete	1.76	0.2	

imum of the considered day. We can observe the important fluctuations of the measured internal temperature around the set point which can be estimated to about ± 0.5 °C, this is due to the control system quality.

Figure 11 shows a comparison between the calculated indoor temperatures with the Bond Graph approach against the experimental data.

A good agreement is observed between the simulated data and the measured ones. The models reproduce properly the thermal behavior represented by the experimental data. Such agreement demonstrates the potential of the new Bond Graph approach and its ability to model the thermal behavior of building systems.

6 Conclusion

In this paper a pseudo-Bond Graph model for one-dimensional transient heat conduction through plane walls has been developed. Two kinds of test problems, regarding boundary conditions, have been selected: the first heat conduction problem involving two different convective conditions at each boundary surface of the wall, which represents a roof or a vertical wall in a building; the second problem dealing with heat conduction in a wall that is subjected to one convective condition at one boundary surface and a fixed temperature condition at the other side, this mimicking heat transfer in a slab.

In such a model, a “lumped” capacity assumption has been adopted with decompo-

sition of the wall into several layers. The resulting pseudo-Bond Graph method has displayed a good capability to reproduce analytical solutions with the possibility to increase the accuracy of the results by adding supplementary layers.

Subsequently, distinct wall pseudo-Bond Graph models have been assembled in a single building model in order to simulate and analyze the overall building thermal behavior. Application of this model has shown satisfactory results. Indeed, the calculated indoor temperatures with Bond Graph model are very close to those measured experimentally.

Future work shall be devoted to update the model to account for radiations exchange (including solar gains) in a way close to reality as discussed for instance by Weiner and Cellier (1993) and Yu and Van Passeen (2004).

References

Borutzky W. (2010): *Bond Graph methodology: Development and Analysis of Multidisciplinary Dynamic System Models*. Springer-Verlag, London. ISBN: 978-1-84882-881-0.

Cellier, F.E.; Nebot, A. (2006): Bond Graph modelling of heat and humidity budgets of Biosphere 2. *Environmental modeling and software*, vol. 21, pp. 1598-1606.

Deque F.; Olivier F.; Poblador A. (2000): Grey boxes used to represent buildings with a minimum number of geometric and thermal parameters. *Energy and Buildings*, vol. 31, pp. 29–35.

Gouda, M.M.; Danaher, S.; Underwood, C.P. (2002): Building thermal model reduction using nonlinear constrained optimization. *Building and environment*, vol. 37, pp. 1255-1265.

Karnopp, D.; Rosenberg, R. (1990): *System dynamics: A unified approach*. Wiley Intersciences New York.

Lorenz, F. ; Massy, G. (1985): *Méthode d'évaluation de l'économie d'énergie apportée par l'intermittence du chauffage dans les bâtiments. Traitement par différences finies d'un modèle à deux constantes de temps*. Rapport No. GM820130-01. Faculté des sciences appliquées, université de Liège, Liège, Belgium (in French).

Nebot, A.; Cellier, F.E. (1999): Simulation of heat and humidity budgets of Biosphere 2 without air conditioning. *Ecological engineering*, vol. 13, pp. 333-356.

Özisik, M.N. (1993): *Heat Conduction*. 2nd edition, Wiley, New York. ISBN: 0-471-53256-8.

Paynter, N. (1961): *Analysis and design of engineering systems*. MIT Press.

Sohlberg, B. (2003): Grey box modeling for model predictive control of heating process. *Journal of Process Control*, vol. 13, pp. 225–38.

Tindale, A. (1999): Third-order lumped parameter simulation method. Building Services Engineering. *Research & Technology*, vol. 14, pp. 87-97.

Weiner, M.; Cellier, F.E. (1993): Modeling and simulation of a solar energy system by use of Bond Graph. Proc. 1st SCS inH. *Conference on Bond Graph modeling and simulation, San Diego, CA*, pp. 301-306.

Yu, B.; Van Paasseen, A.H.C. (2004): Simulink and Bond Graph modeling of an air-conditioning room. *Simulation modeling Practice and theory*, vol. 12, pp. 61-76.